

NASA Technical Memorandum 100847

# Advanced Sensible Heat Solar Receiver for Space Power

(NASA-TM-100847) ADVANCED SENSIBLE HEAT  
SOLAR RECEIVER FOR SPACE POWER (NASA) 12 p  
CSCL 10B

N88-21249

Unclas  
G3/20 0136324

Timothy J. Bennett  
*Sverdrup Technology, Inc.*  
*(Lewis Research Center Group)*  
*NASA Lewis Research Center*  
*Cleveland, Ohio*

and

Dovie E. Lacy  
*NASA Lewis Research Center*  
*Cleveland, Ohio*

Prepared for the  
23rd Intersociety Energy Conversion Engineering Conference  
cosponsored by the ASME, AIAA, ANS, SAE, IEEE, ASC, and AIChE  
Denver, Colorado, July 31—August 5, 1988



## ADVANCED SENSIBLE HEAT SOLAR RECEIVER FOR SPACE POWER

Timothy J. Bennett  
Sverdrup Technology, Inc  
(Lewis Research Center Group)  
NASA Lewis Research Center  
Cleveland, Ohio 44135

and

Dovie E. Lacy  
National Aeronautics and Space Administration  
Lewis Research Center  
Cleveland, Ohio 44135

### ABSTRACT

NASA Lewis through in-house efforts has initiated a study to generate a conceptual design of a sensible heat solar receiver and to determine the feasibility of this system for space power applications. The sensible heat solar receiver generated in this study uses pure lithium as the thermal storage media and was designed for a 7 kWe Brayton (PCS) operating at 1100 K. The receiver consists of two stages interconnected via temperature sensing variable conductance sodium heat pipes. The lithium is contained within a niobium vessel and the outer shell of the receiver is constructed of third generation rigid, fibrous ceramic insulation material. Reradiation losses are controlled with niobium and aluminum shields. By nature of design, the sensible heat receiver generated in this study is comparable in both size and mass to a latent heat system of similar thermal capacitance. The heat receiver design and thermal analysis was conducted through the combined use of PATRAN, SINDA, TRASYS, and NASTRAN software packages.

### INTRODUCTION

Solar dynamic power systems are currently being studied as a means of providing electrical power for space applications. One of the key components in the solar dynamic power system is the heat receiver/thermal energy storage (TES) sub-system. The state of the art (SOA) heat receiver/TES sub-system is one of the larger and heavier components in the solar dynamic power system; and the upper operating temperature is limited by reradiation losses from the aperture. Therefore, future design and development of advanced solar dynamic power systems will be directed toward concepts that are more efficient and lighter than the SOA.

The need to investigate sensible heat storage technology stems from the uncertainties associated with latent heat storage materials, more specifically phase change salts. In recent latent heat receiver designs lithium salts such as, lithium fluoride and lithium hydroxide have been used and the problems which they present have yet to be resolved. Although

these salts have relatively high heats of fusion, they also have very low thermal conductivities, low densities, high volume expansion upon melting, and are very corrosive. Thus, the resulting heat receiver/thermal energy storage sub-system is large and massive due to required thermal conductivity enhancing devices and additional containment material (1).

However, sensible heat storage systems, utilizing liquid lithium as the storage media, possess the capability to improve upon or minimize these problems. In sensible heat storage systems volume change can be limited by controlling the magnitude of the associated temperature swings; a smaller temperature change will result in a smaller volume change thus, a smaller void will be produced. Lithium has a much higher thermal conductivity and is not as corrosive as the lithium salts. Therefore, thermal conductivity enhancing devices are not needed and the life expectancy of the containment vessel is increased. In the past, sensible heat receiver concepts have been much larger and more massive than latent heat systems due to the amount of additional material required to store equivalent amounts of energy. However, the sensible heat receiver designed in this study is comparable in both size and mass to a latent heat system of similar thermal capacitance.

### DESIGN REQUIREMENTS

The design requirements shown in Table I for the sensible heat receiver are similar to those specified for earlier latent heat receiver studies (2). The only difference is the thermal storage media. The objective of the sensible heat receiver study was to generate and evaluate a conceptual design for a liquid lithium solar dynamic heat receiver for a Brayton space power system. A point design of 7 kWe was selected for this study, but the concept is to be applicable to a variety of power levels ranging from 1.5 to 50 kWe.

In addition to the specified design requirements, the sensible heat receiver design was to include:

- (1) an optimized aperture
- (2) an optimized cavity geometry
- (3) an insulated outer shell

- (4) tubular heat transfer surfaces
- (5) maximum heat exchanger pressure drop of 4 percent
- (6) inlet working fluid pressure of 60 psi

The output from the study was to include as a minimum:

- (1) material selections
- (2) mass and size
- (3) thermal performance parameters at start-up
- (4) orbital steady state operation
- (5) structural requirements

#### LITHIUM SENSIBLE HEAT RECEIVER DESIGN

The sensible heat receiver shown in Fig. 1 consists of two stages, one to store sensible thermal energy, and the other to supply the Brayton cycle working fluid with a uniform heat input. The thermal storage or upper stage, receives solar energy from the concentrator and stores it in a lithium bath. Energy is transferred to the lower stage via temperature sensing variable conductance heat pipes (TSVCHP).

##### Upper Stage Design

Design of the upper stage focused primarily on optimizing the aperture diameter and the receiver's internal configuration. The aperture had to be large enough to allow an optimum amount of concentrated solar energy to reach the receiver cavity and small enough to minimize reradiation losses. In this study the maximum aperture diameter was limited to 14.6 cm which is the diameter of the focused concentrator image. Optimization of the aperture also involved selecting a diameter which balanced gains and losses to produce a predetermined peak operating temperature for the cavity skin. The final heat receiver design required a aperture diameter of 13.3 cm.

Optimization of the receiver's cavity included minimizing aperture losses and thermal stresses, and considerations for the ease with which the receiver could be manufactured. Four different cavity geometries were analyzed. Through varying heights and radii, the condition which produced minimum radiation exchange between the cavity and the aperture was determined. The receiver cavity shapes analyzed for this study were: hemispherical base with a cylindrical top, Fig. 2(a); hemispherical base with a conical top, Fig. 2(b); hemispherical base and a cylindrical top with a cone centered on the base, Fig. 2(c); and a cylinder, Fig. 2(d). For Figs. 2(a) and (b), the height of the upper portion of the cavity (cylindrical or conical section) was varied according to the radius of the lower hemisphere, so that the incoming solar flux was evenly distributed only on the lower hemispherical surface.

The cylindrical shape (Fig. 2(d)) produced the lowest AF values ( $\alpha_{\text{cAF}}$ ) between the cavity and the aperture but, the shape was assumed to have high thermal stresses which translate into low life expectancy. The AF values for the other three configurations were found to be nearly equal. The configuration with the hemispherical base and cylindrical top (Fig. 2(a)) was considered to have the lowest thermal stress and provided ease of manufacturing therefore, it was selected as the receiver's upper stage cavity geometry.

The amount of lithium required for the receiver's upper stage is based on a specified operating temperature for the power cycle, the maximum upper operating temperature, and the total reradiation and external surface losses. The initial design goals for this

program were: a temperature range of 139 to 167 K, an upper operating temperature of 1500 K, and a 20 percent loss rate. It was estimated that 136 kg of lithium would be required to meet these design goals. Also, the upper stage was designed to have a relatively equal cross sectional area of lithium in order to provide even heating and reduce thermal gradients.

##### Lower Stage Design

The lower stage is designed to provide a constant supply of energy to the helium/xenon working fluid at a constant temperature. The ringed configuration of the lower stage minimizes the weight of the receiver by minimizing the amount of lithium (which provides damping for temperature fluctuations) required. It would be possible to eliminate the lithium in the lower stage if the turbine could accept larger temperature fluctuations. The heat exchanger is constructed of six 3.6 cm ID niobium tubes with 0.159 cm walls, and a length of 0.9 m. The tubes are attached to a 8.89 cm inlet and outlet header (Fig. 1). This heat exchanger design provides a 3 percent pressure drop and requires a 166.7 K temperature difference between the lithium and the working fluid to produce an exit temperature of 1100 K.

Due to the high operating temperature and erosive nature of lithium, the selection of a containment material was limited to only a few metals; molybdenum alloys, tantalum alloys, and niobium. After a review of these materials, 0.1 inch skins of niobium was selected for containment of both the upper and lower stages. This selection was made based on the low density and the workability of niobium. Table II contains mass information based on material selection and component, and figure 3 is a pictorial representation of the temperatures associated with the various receiver materials.

##### Heat Pipe Operation

The temperature sensing variable conductance heat pipe (TSVCHP) transfers heat from the upper stage to the lower stage. The TSVCHP used in this study differs from a standard variable conductance heat pipe (VCHP), in that the VCHP maintains a constant evaporation side temperature and the TSVCHP maintains a constant condenser side temperature. The design of the TSVCHP requires a processor, two temperature sensors, and a gas reserve with resistance heating, Fig. 4. The first sensor monitors the exiting working fluid temperature and the second monitors the upper stage lithium temperature. As the temperature of the working fluid increases or decreases, the first sensor provides feedback to the processor which either increases or decreases the electrical energy supplied to the resistance heater in the gas reserve. This in turn varies the pressure of the inert gas. Increasing the pressure decreases the conductance of the heat pipe by filling the condensing end of the heat pipe with gas. The second sensor provides information to the processor such that compensation is made for a change in the vapor pressure of the sodium heat pipe caused by a change in the temperature of the upper stage lithium. Increasing the upper stage temperature increases the vapor pressure of the sodium. A greater sodium vapor pressure requires a greater pressure in the gas reserve to maintain the same gas level in the condenser portion of the heat pipe.

To start transferring heat from the upper stage to the lower stage, via the heat pipe, the lithium surrounding the heat pipe must reach a temperature of 778 K, which is the minimum operating temperature of

a sodium heat pipe. If the lithium in the upper stage, surrounding the heat pipe, exceeded 1573 K or fell below 778 K the heat pipe would cease to operate. Once the upper stage reaches a minimum temperature of 1500 K and the lower stage reaches a temperature of 1100 K, the working fluid begins circulating.

#### Heat Receiver Structure

The lithium vessels are contained within a cylindrical structure of High Thermal Performance (HTP) ceramic insulation, with a void space maintaining separation between the upper and lower vessels and the casing, see Fig. 1. The vessels are structurally separated from one another and the HTP insulation by thin HTP standoffs. The entire receiver is encased in a thin shell of titanium to provide an attachment surface for fastening the receiver to the concentrator and other structures. A list of HTP materials properties are shown in Table III.

#### HEAT RECEIVER ANALYSIS

Four software packages were used to analyze the heat receiver: PATRAN and associated programs, SINDA, TRASYS and NASTRAN. PATRAN was used as a pre-processor to generate a three-dimensional model of the receiver to be translated into SINDA and NASTRAN input decks, and as a post-processor to show thermal and stress contours.

TRASYS is used to calculate the AF values for internal and external surfaces, and to generate solar, albedo, and planetary gains on the outer surface. Figure 5 shows time slices for a typical low earth orbit application and Fig. 6 shows the associated gains on the receiver surface and cavity. Gains on the cavity from the concentrator are calculated using the solar constant and concentrator data. Except for the bottom surface, the sink temperature for all external surfaces and the aperture is absolute zero. The bottom radiation sink temperature was set at 945 K due to its view of the Brayton turbine, which operates at a temperature of 1100 K.

The receiver is symmetrical in the theta direction, and it is assumed that the solar beam from the concentrator is evenly distributed over the hemispherical cavity. Also, the assumption is made that the concentrator is not shadowed from the other objects. Because of symmetry, a one sixtieth section in the theta direction was modeled, using 519 nodes and providing an approximate maximum 2.6 cm grid line in any direction. The need for detailed temperature profiles requires the use of a fine grid. The conductivity of the heat pipe was controlled by checking the working fluid temperature to determine the amount of heat needed. The amount of heat required was extracted from five nodes in the upper section and added to five nodes in the lower section. Heat transfer from the upper to the lower stage through the heat pipe casing was ignored. It was assumed that the amount of heat transferred in this manner would be balanced by a decrease in the amount transferred through the sodium. The heat transfer from the heat exchanger header pipes to space was also ignored based on the assumption that the tubes were well insulated, and the simplicity of the model.

#### Start Up Operation

At start-up, it is assumed that the receiver is at orbital steady state with its environment. In Fig. 7 the steady state, first, third, and sixth

orbits are shown. At the end of the first sunlit portion, where the concentrator is first aligned with the receiver, the upper stage vessel temperature raises to 826 K, the outer components of the receiver range from 718 K to 772 K. During the third orbit of the sunlit portion the sodium heat pipes start transferring energy to the lower stage. In the sixth orbit, the upper and lower stages have reached the minimum start-up temperatures and the working fluid starts circulating. By the end of the sixth orbit the lower stage is in a steady state condition. Several additional orbits are required before the upper stage has cooled down to its orbital steady state condition.

#### Transient Operation

The four pictures shown in Fig. 8 represent different times in a typical orbit. In Fig. 8(a) the receiver is at midpoint of the sunlit portion of the orbit, located between the sun and earth. Figure 8(b) represents the end of the sunlit portion, where the upper stage is at its maximum operating temperature. Figure 8(c) is midway through the eclipse portion, and Fig. 8(d) represents temperatures at the end of the eclipse portion of the orbit. Throughout the orbit the upper stage temperature varies from 1311 to 1527 K, while the lower stage maintains a constant temperature of 1102 K. In Fig. 8(d) the lithium around the heat pipe on the evaporator side is at the same temperature as the lithium surrounding the condenser portion of the heat pipe. At this point the heat pipe ceases to transfer heat and the effects of this is shown in Fig. 9. As indicated the working fluid temperature drops to 1098 K, which is still within the  $\pm 4$  K temperature error limit. The system energy balance for a typical orbit is given in Table IV.

#### CONCLUDING REMARKS

The sensible heat receiver compares well with the 7 kWe latent heat receivers analyzed in earlier studies, and it satisfies the specified design requirements. Table V represents a comparison between the sensible heat receiver discussed herein and several latent heat receiver concepts. The weight and size of the sensible receiver can be further reduced by optimizing the niobium skin thickness, and by minimizing or eliminating the lower stage lithium. The life stress analysis performed for the niobium vessels indicate that the material is capable of maintaining structural integrity for 7 to 10 yrs operating at 1100 to 1400 K. Finally, the concept can be sized for different power requirements by increasing or decreasing the size and incorporating a movable aperture plate.

#### REFERENCES

1. Lacy, D.E., Coles-Hamilton, C., and Juhasz, A., 1987, "Selection of High Temperature Thermal Energy Storage Materials for Advanced Solar Dynamic Space Power Systems," NASA TM-89886.
2. Strumpf, H., and Coombs, M., 1987, "Advanced Heat Receiver Conceptual Design Study," NASA CR-180901.

TABLE I. - HEAT RECEIVER DESIGN REQUIREMENTS

<u>Brayton cycles:</u>	
Turbine inlet temperature, K . . . . .	1100±4
Working fluid . . . . .	He/Xe
Working fluid molecular wt . . . . .	40
Brayton cycle efficiency, percent . . . . .	30
Electrical power output, kWe . . . . .	7
<u>Solar concentrator:</u>	
Type . . . . .	Parabolic
Concentrator efficiency, percent . . . . .	90
Concentration ratio . . . . .	3000
Rim angle, deg . . . . .	60
Diameter, m . . . . .	8
Surface accuracy, mrad . . . . .	1
<u>Orbit:</u>	
Circular, km . . . . .	463.5
Period, min . . . . .	93.6
Eclipse, min . . . . .	36
Solar constant, kw/m <sup>2</sup> . . . . .	1.371

TABLE II. - MASS AND MATERIAL SUMMARY

Component	Mass, kg
Upper stage storage container, niobium	90
Lower stage storage container, niobium	38
Upper stage lithium	136
Lower stage lithium	38
Heat exchanger, niobium	18
Outer cylindrical structure, titanium	28
Sodium heat pipes, niobium casing	9
Insulation, HTP-12	45
Mounting hardware	4
	<u>406</u>

TABLE III. - HIGH THERMAL PERFORMANCE (HTP) INSULATION PROPERTIES

Properties	
Main components	
Alumina fibers, wt %	22
Silica fibers, wt %	78
Density, kg/m <sup>3</sup>	192
Tension in plane, kPa	2206
Compression through tension, kPa	972
Dielectric constant	1.22
Loss tangent	0.0010
Thermal conductivity, W/m•K (1260 °C)	0.124
Coefficient of expansion, cm/cm-Cx10 <sup>-7</sup>	25.56
Long cycle life at, °C	1427
Limited exposure to, °C	1593
Manufacturer	Lockheed Missiles and Space

TABLE IV. - TYPICAL ORBIT ENERGY BALANCE

Orbit time, hr	Percent losses		Percent to fluid
	Surface	Aperture	
0.00	10.48	14.16	75.36
.13	12.64	14.34	73.02
.26	15.80	41.30	69.90
.39	18.84	14.23	66.93
.52	19.00	13.03	67.97
.65	18.67	11.95	69.38
.78	18.09	11.21	70.70
.91	17.60	10.55	71.85
1.04	16.67	10.03	73.30
1.17	15.84	11.49	72.67
1.30	12.74	12.58	74.68
1.43	10.61	13.45	75.94
1.52	10.43	14.04	75.53
Average	15.19	12.72	72.09

TABLE V. - 7 kWe BRAYTON RECEIVER SIZE SUMMARY

Configuration	Receiver mass, kg	Receiver O.D., m	Receiver length, m	Receiver volume, m <sup>3</sup>
Baseline <sup>a</sup>	443	1.15	2.08	2.160
Packed bed <sup>a</sup>	280	.90	1.30	.840
Plate-fin <sup>a</sup>	367	.94	1.98	1.380
Heat pipe <sup>a</sup>	304	.73	1.25	.520
Sensible heat	406	1.14	1.09	1.110

<sup>a</sup>Obtained from Ref. 2.

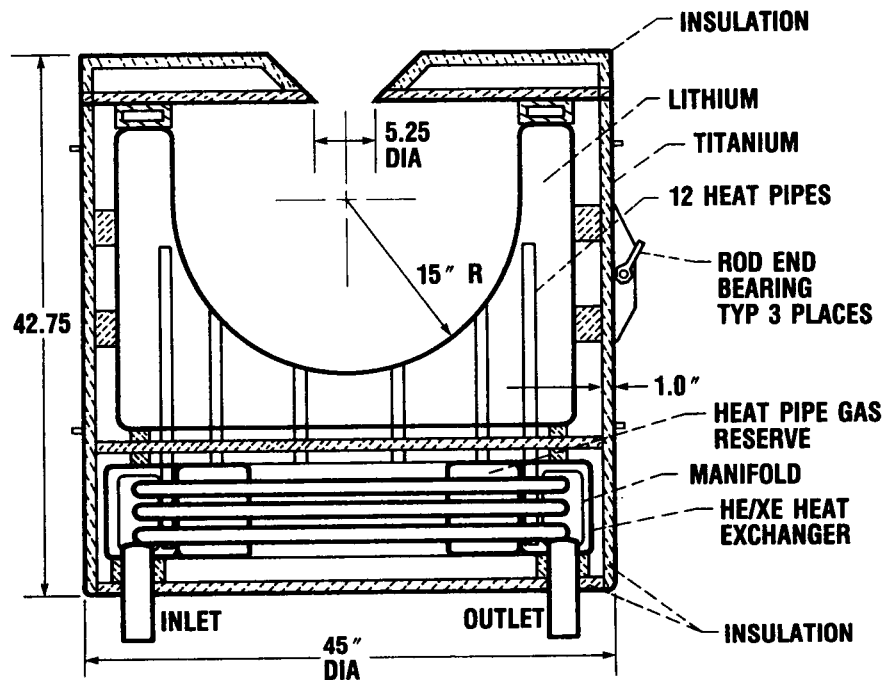


FIGURE 1. - SENSIBLE HEAT RECEIVER CONFIGURATION.

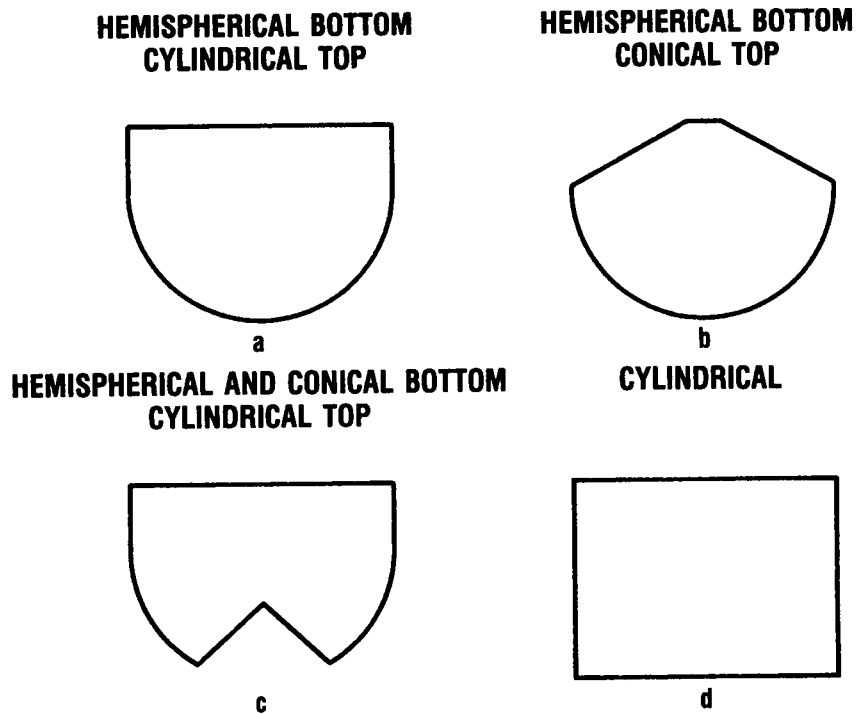


FIGURE 2. - GEOMETRIC SHAPES FOR CAVITY DESIGN.

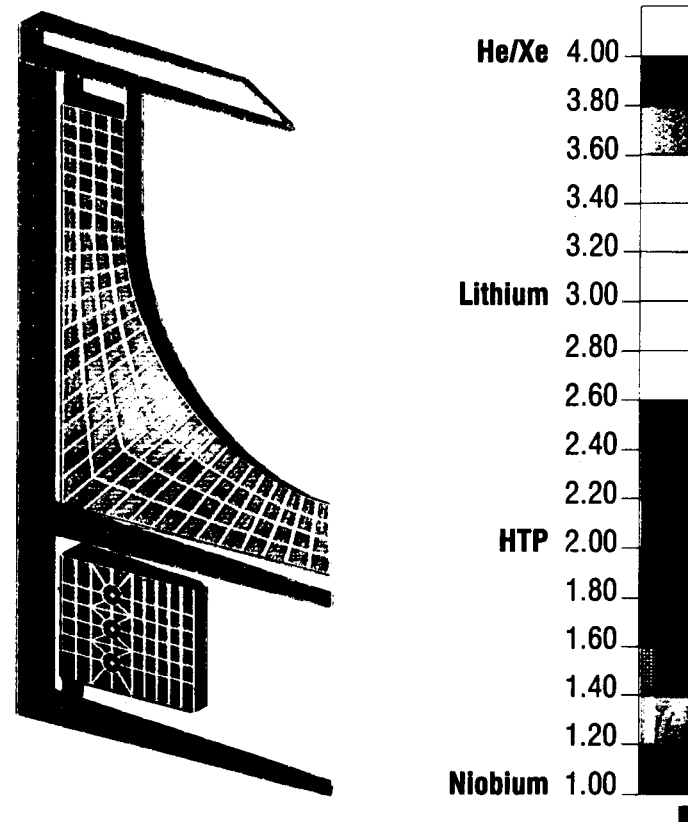


FIGURE 3. - RECEIVER MATERIAL PROFILE.

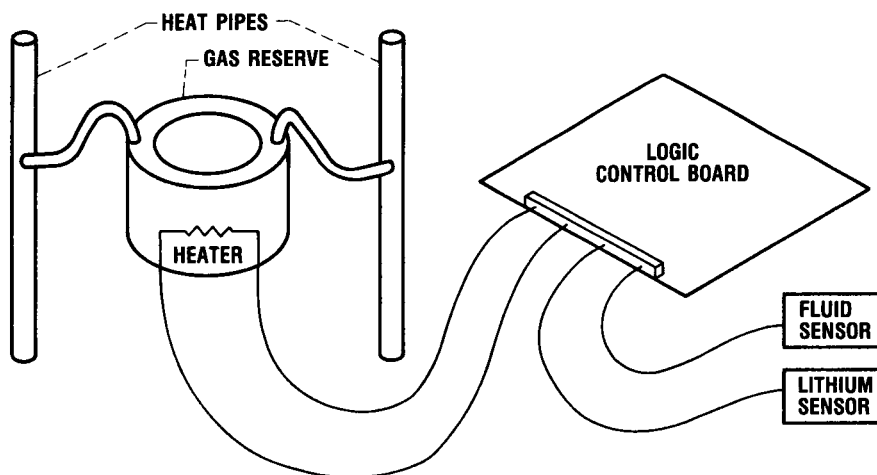


FIGURE 4. - TEMPERATURE SENSING VARIABLE CONDUCTANCE HEAT PIPE CONFIGURATION.



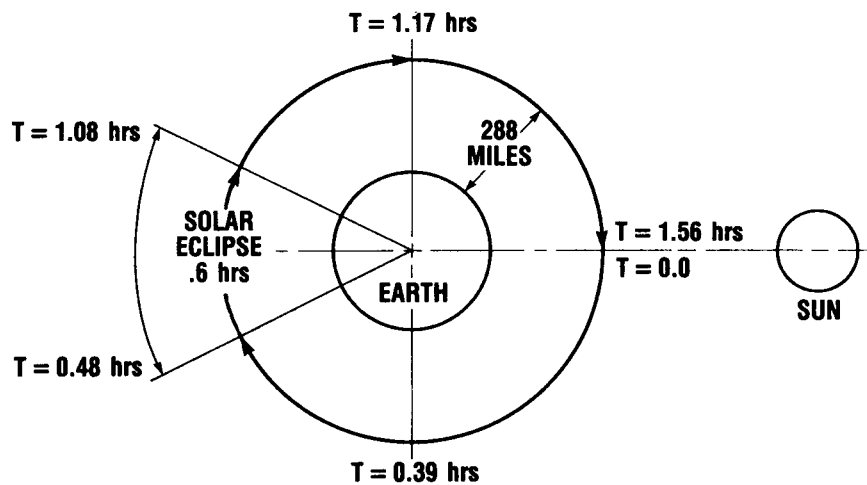


FIGURE 5. - TIME SLICES FOR A TYPICAL LOW EARTH ORBIT APPLICATION.

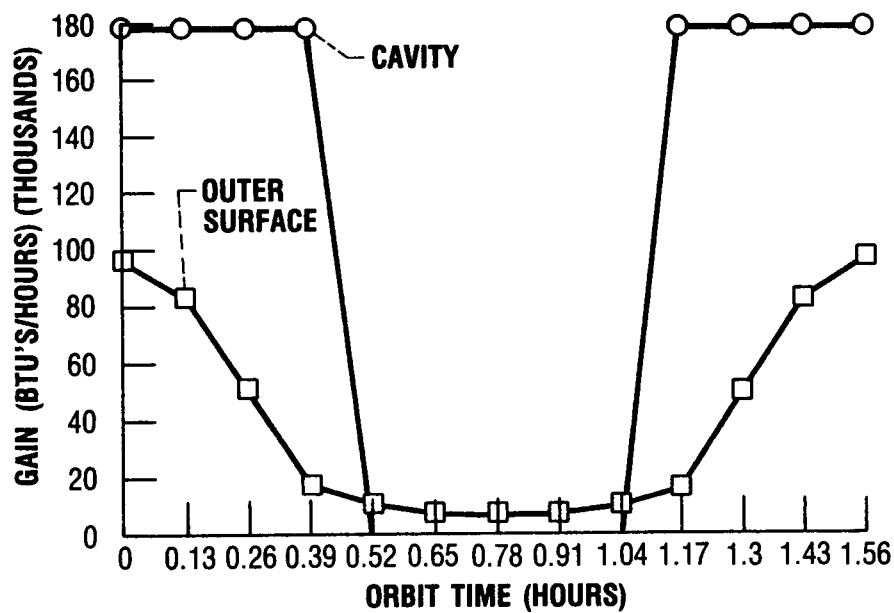


FIGURE 6. - SOLAR, ALBEDO AND PLANETARY GAINS.

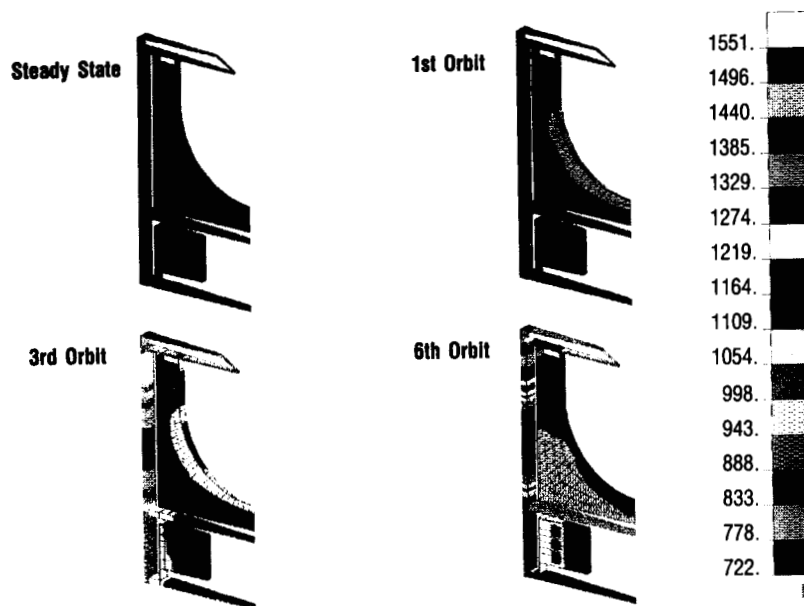


FIGURE 7. - THERMAL PROFILE FOR START-UP OPERATION.

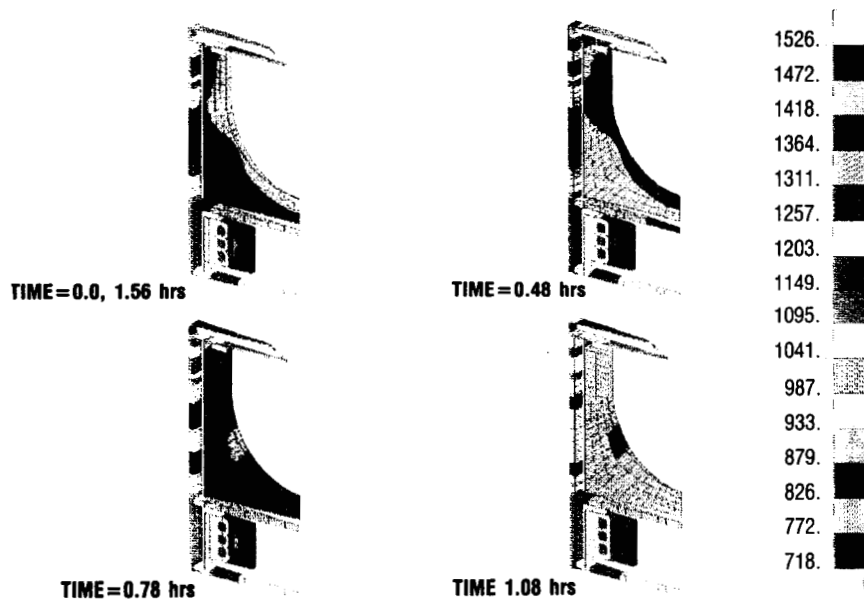


FIGURE 8. - THERMAL PROFILE FOR A TYPICAL ORBIT.

ORIGINAL PAGE IS  
OF POOR QUALITY

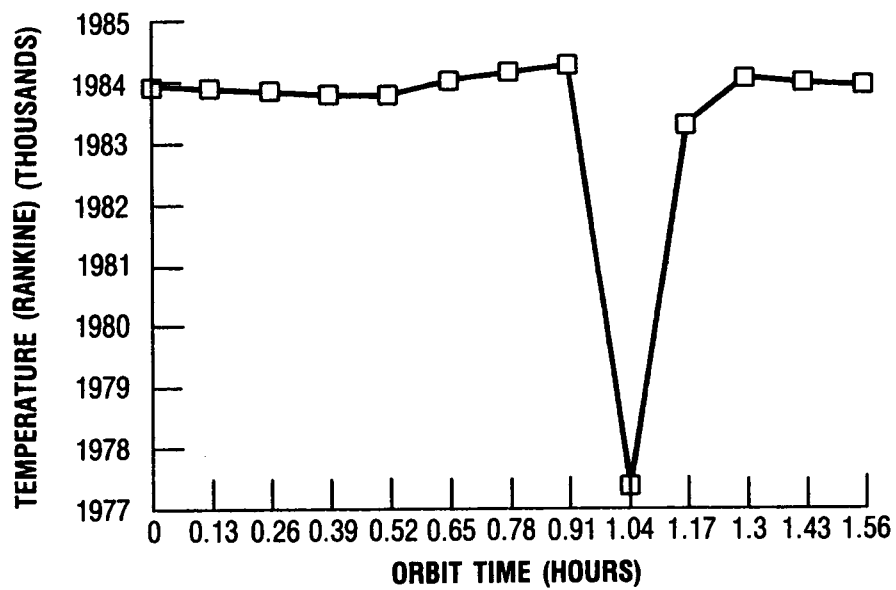


FIGURE 9. - WORKING FLUID TEMPERATURE AS A FUNCTION OF TIME.

# Report Documentation Page

1. Report No.  NASA TM-100847		2. Government Accession No.		3. Recipient's Catalog No.	
4. Title and Subtitle  Advanced Sensible Heat Solar Receiver For Space Power				5. Report Date	
				6. Performing Organization Code	
7. Author(s)  Timothy J. Bennett and Dovie E. Lacy				8. Performing Organization Report No.  E-4008	
				10. Work Unit No.  506-41-31	
9. Performing Organization Name and Address  National Aeronautics and Space Administration Lewis Research Center Cleveland, Ohio 44135-3191				11. Contract or Grant No.	
				13. Type of Report and Period Covered  Technical Memorandum	
12. Sponsoring Agency Name and Address  National Aeronautics and Space Administration Washington, D.C. 20546-0001				14. Sponsoring Agency Code	
15. Supplementary Notes Prepared for the 23rd Intersociety Energy Conversion Engineering Conference cosponsored by the ASME, AIAA, ANS, SAE, IEEE, ACS, and AIChE, Denver, Colorado, July 31 - August 5, 1988. Timothy J. Bennett, Sverdrup Technology, Inc. (Lewis Research Center Group), NASA Lewis Research Center; Dovie E. Lacy, NASA Lewis Research Center.					
16. Abstract  NASA Lewis through in-house efforts has begun a study to generate a conceptual design of a sensible heat solar receiver and to determine the feasibility of such a system for space power applications. The sensible heat solar receiver generated in this study uses pure lithium as the thermal storage media and was designed for a 7 kWe Brayton (PCS) operating at 1100 K. The receiver consists of two stages interconnected via temperature sensing variable conductance sodium heat pipes. The lithium is contained within a niobium vessel and the outer shell of the receiver is constructed of third generation rigid, fibrous ceramic insulation material. Reradiation losses are controlled with niobium and aluminum shields. By nature of design, the sensible heat receiver generated in this study is comparable in both size and mass to a latent heat system of similar thermal capacitance. The heat receiver design and thermal analysis was conducted through the combined use of PATRAN, SINDA, TRASYS, and NASTRAN software packages.					
17. Key Words (Suggested by Author(s))  Solar dynamic, Brayton, Lithium, Sensible heat, Receiver, Thermal storage, High temperature				18. Distribution Statement  Unclassified - Unlimited Subject Category 20	
19. Security Classif. (of this report)  Unclassified		20. Security Classif. (of this page)  Unclassified		21. No of pages  12	
				22. Price*  A02	